Available online at www.sciencedirect.com
ScienceDirect
European Polymer Journal 43 (2007) 4750–4761
EUROPEAN POLYMER JOURNAL
www.elsevier.com/locate/europolj

Effects of annealing treatment on the properties of MEH-PPV/titania hybrids prepared via *in situ* sol–gel reaction

Hung-Jen Chen [a], Leeyih Wang [b,c,*], Wen-Yen Chiu [a,b,*]

[a] *Department of Chemical Engineering, National Taiwan University, Taipei, Taiwan, ROC*
[b] *Institute of Polymer Science and Engineering, National Taiwan University, Taiwan, ROC*
[c] *Center for Condensed Matter Sciences, National Taiwan University, Taiwan, ROC*

Received 12 February 2007; received in revised form 28 July 2007; accepted 6 August 2007
Available online 19 August 2007

Abstract

A uniform poly[2-methoxy-5-(2′-ethylhexyloxy)-*p*-phenylenevinylene] (MEH-PPV)/titania hybrid film was successfully prepared by an *in situ* sol–gel reaction of titanium isopropoxide (TIP) in the presence of MEH-PPV/2-chlorophenol solution. The annealing treatment increased the conversion of TIP to titania as determined from evidence of the formation of Ti–O–Ti bonds in the Fourier transform infrared (FTIR) spectrum. Scanning electronic microscope (SEM) photographs showed that the morphology and distribution of titania in the hybrid film were strongly related to the amount of water in the *in situ* sol–gel reaction. The thermal stability of MEH-PPV/titania hybrids was enhanced by the annealing treatment. Small angle X-ray scattering (SAXS) and X-ray diffraction (XRD) analyses indicated that annealing treatment promoted the ordered aggregation of the MEH-PPV chains and crystallization of titania to a certain extent. The blue shift in Ultraviolet–visible (UV–vis) absorption of pure MEH-PPV after annealing was ascribed to the small extent of decomposition and coil conformation which occurred at high temperature. A more-obvious blue shift for the hybrids was observed, which resulted from irregular aggregation and coil conformation of the MEH-PPV chains induced by heterogeneous point, TIP (titania). The red shift in the photoluminescent (PL) emission for pure MEH-PPV resulted from a certain extent of ordered aggregation after annealing. However, only a slight red shift in the PL emission peak for the hybrids was found due to the hindrance of ordered aggregation of MEH-PPV chains in the presence of TIP (titania).

Keywords: MEH-PPV/titania hybrid; Annealing; Morphology; Properties

1. Introduction

The preparation of organic/inorganic hybrids has received much attention over the past few years [1–3]. The major problem when preparing organic/inorganic hybrids is how to overcome the incompatibilities between the organic and inorganic components. In our previous study, a

* Corresponding authors. Addresses: Center for Condensed Matter Sciences, National Taiwan University, No. 1, Sec. 4, Roosevelt Road, Taipei, Taiwan 106, ROC (L. Wang), Department of Chemical Engineering, National Taiwan University, Taipei, Taiwan, ROC (W.-Y. Chiu). Tel.: +886 2 33665276; fax: +886 2 23655404 (L. Wang), tel./fax: +886 2 2362 3259 (W.-Y. Chiu).
E-mail addresses: leewang@ntu.edu.tw (L. Wang), ycchiu@ntu.edu.tw (W.-Y. Chiu).

0014-3057/$ - see front matter © 2007 Elsevier Ltd. All rights reserved.
doi:10.1016/j.eurpolymj.2007.08.006

homogenous MEH-PPV/titania hybrid was successfully synthesized via *in situ* sol–gel reaction [4]. However, the conversion of titanium alkoxide to titania was not sufficiently high. Annealing treatment is usually required to resolve this problem. It is thought that except for the control in a pre-synthesized condition, processing parameters such as the choice of solvent, spin speed, and annealing treatment also play key roles in determining the film morphology, which in turn affects the film properties [5–10].

Luminescent conjugated polymers are very promising candidates for application to large-area polymer light emitting diodes (PLEDs), field-effect transistors (FETs), and solar cells. This is because their structures can be easily modified, and they can also be fabricated using versatile wet-processing approaches. Among these polymers, MEH-PPV is one of most interesting conjugated polymers due to its excellent electro-optical properties. Numerous studies have focused on the morphological effects for achieving better film properties, in addition to the influence of the molecular structure [11–14]. Annealing treatment greatly influences morphological changes, which mainly result from the rearrangement of polymer chains [8–10]. Polymer interchain interactions and the corresponding formation of aggregates, polaron pairs, and excimers are all responsible for quenching the quantum yield [12,15] and changing the electro-optical properties.

When applying PLEDs, several attempts have been made to suppress the formation of aggregation. For example, an efficient method is blending with a high-T_g polymer to limit chain mobility and correspondingly avoid aggregation [16,17]. Another approach to preventing aggregation of polymer chains is to use inorganic pendent groups as a side chain of the conjugated polymer [18,19]. Nevertheless, a certain degree of aggregation still exists in MEH-PPV films, dependent on the solvent, concentration, spin rate, and especially the annealing treatment [5,9,10]. Improvements in the quantum efficiency based on annealing treatments should be carefully controlled at an appropriate temperature [6].

Although aggregation induced by annealing will lower the quantum efficiency, it enhances mobility, which is required for FETs and solar cells. Breemen et al. showed that the mobility of symmetrically substituted poly(*p*-phenylene vinylene) (PPV) derivatives can be improved to a value of 10^{-2} cm^2 V^{-1} s^{-1} by annealing treatment, which is as high as highly regioregular head-to-tail poly(3-hexyl thiophene) [20]. Another important purpose of annealing treatment is to facilitate the polymer reaching an equilibrium state. The most frequently used method for fabricating polymer devices is spin-coating. However, the high solvent evaporation rate during spin-coating freezes the state of the polymer chains, which is far from their equilibrium state. From the viewpoint of thermodynamics, there are strong forces driving the reorganization of the molecular morphology to a more-stable state. This reorganization will have a significant effect on the performance and long-term stability of a device [21]. Promoting polymers reach an equilibrium state at an elevated temperature is an important function of annealing treatment [22].

Titania is widely used as an electron acceptor in organic solar cell applications due to its excellent electro-optical properties. In order to control the phase separation of polymer/titania hybrids in the nanometer range, *in situ* sol–gel reaction is a useful technique. Janssen et al. reported an air sol–gel reaction for preparing poly[2-methoxy-5-(3′,7′-dimethyloctyloxy)-*p*-phenylenevinylene] (MDMO-PPV)/titania bulk-heterojunction hybrids [23] by spin-coating a mixture of titania isopropoxide and MDMO-PPV, followed subsequently by the sol–gel reaction in a humid environment. The performance of this air sol–gel MDMO-PPV/titania hybrid is significantly affected by environment conditions [24]. In addition, the efficiency is apparently limited by the amorphous state of titania. To improve the electron mobility, a nanocrystalline structure is necessary. Therefore, another polymer/semiconducting particle hybrid was developed using zinc alkoxide due to the fact that nanocrystalline ZnO can be obtained at a moderate temperature of 110 °C, which does not destroy the structure of the polymer component [25]. It should be noted that a relatively high temperature of >350 °C [26] is required to obtain nanocrystalline TiO_2, yet this high temperature degrades the organic component.

There are currently increasing numbers of studies focusing on low-temperature sintering processes to prepare nanocrystalline TiO_2 onto plastic substrates [27,28]. In this work, the influence of the annealing treatment on the morphological and structural characteristics of MEH-PPV and titania was investigated. Relationships among the morphology, structure, and properties are fully discussed.

2. Experiment

2.1. Materials

Titanium (IV) isopropoxide (TIP) and 2-chlorophenol (2-CP) were used as received. The water used in the sol–gel reaction was purified using a Millipore Milli-Q system. The weight-average molecular weight (M_w) of MEH-PPV was about 600,000 as determined by gel permeation chromatography (GPC), which was calibrated using polystyrene standard.

2.2. Preparation of MEH-PPV/titania (TIP) hybrid

2.2.1. Explanation of notation

Table 1 shows the reagents and their amounts used in the preparation of MEH-PPV/titania (TIP) hybrids. The notation is explained by selecting "hy-W4" as an example. The first term, hy, means a hybrid; the second term, W, refers to water, and 4 represents the molar ratio of water to TIP. The weight ratio of TIP to (TIP + MEH-PPV) in the hybrid was fixed at 60.3 wt%, and the concentration of MEH-PPV in the solvent, 2-CP, was fixed at 5 mg/ml (0.5% w/v).

2.2.2. In situ sol–gel reaction

A 100-ml round-bottomed flask equipped with a stirrer and condenser was used. In a typical procedure, the desired amount of TIP was fully dissolved in a premixed solution containing MEH-PPV and 2-CP. After 30 min of stirring, a quantitative amount of water was added drop-wise to the MEH-PPV/TIP solution. The sol–gel reaction was first carried out at room temperature for 30 min and then at 90 °C for 10 h. The appearances of the final MEH-PPV/titania (TIP) hybrid solutions are described in Table 1.

2.3. Specimen preparation and measurements

2.3.1. Process for ITO cleaning and annealing treatment

The indium tin oxide (ITO) glass (10 Ω/□, Ritek, Taiwan) was subjected to a routine cleaning process [4]. MEH-PPV/titania (TIP) hybrid solutions were spun onto ITO glass at 3000 rpm. The hybrid film was annealed at a 2 °C/min heating rate from room temperature to the desired annealing temperature and then remained at the annealing temperature for 1 h. At completion of the annealing treatment, the solution was rapidly cooled to room temperature. The annealing treatment was carried out under a protective flow of nitrogen gas and was kept away from light.

2.3.2. FTIR measurement

The functional groups and interactions of MEH-PPV, TIP, 2-CP, and hybrids were analyzed by a Fourier transform infrared spectrophotometer (FTIR) (Bio-Rad, FTS-3000). Specimens were prepared by coating the hybrid solutions on potassium bromide (KBr) pellets and drying out the solvent. The absorption spectra were recorded with 16 scans at a resolution of 4 cm^{-1} between 1800 and 400 cm^{-1}.

2.3.3. SEM photograph

The aggregate size and aggregation phenomena of MEH-PPV/titania (TIP) hybrid films were observed using a Hitachi (S-800) scanning electronic microscope (SEM) at an activation voltage of 20 kV.

2.3.4. UV–vis measurement

The Ultraviolet–visible (UV–vis) absorption of all hybrid films was performed using a UV–vis spectrometer (Thermo Spectronic gamma series).

2.3.5. PL measurement

Photoluminescent (PL) studies of hybrid films were recorded on a Fluorolog-Tau-3 spectrometer (Jobin Yvon) using a xenon lamp for the excitation source with photoexcitation at 502 nm.

2.3.6. SAXS and XRD measurement

Small angle X-ray scattering (PSAXS-USH-WAXS-002; Osmic), using Cu Kα radiation at 45 kV and 0.67 mA, was used to investigate the morphology of MEH-PPV in the hybrids. The test

Table 1
Composition and appearance of the MEH-PPV/TIP hybrid solutions

	H_2O/TIP (mole ratio)	TIP/hybrid (wt%)	Concentration (mg/ml)	Appearance
hy-W4	4	60.3	5	Clear
hy-W16	16	60.3	5	Clear
hy-W200	200	60.3	5	Turbid

samples were prepared by detaching them from the glass substrate and sticking them onto 3 M tape. The X-ray diffraction study (MXP-3; MAC Science Diffractometer), using Cu Kα radiation at 40 kV and 30 mA, was conducted to examine the crystalline patterns of MEH-PPV/titania (TIP) hybrids. The measured specimens were ground into a powder form for the analysis.

2.3.7. TGA measurement

A thermogravimetric analyzer (TGA) from Perkin Elmer (TGA-7) was used to examine the thermal degradation behavior of MEH-PPV/titania (TIP) hybrids. Specimens of 5–15 mg of ground-up powder were put into a platinum crucible and heated at a rate of 10 °C/min under a nitrogen atmosphere. The recorded temperature was from 100 to 800 °C.

3. Results and discussion

3.1. FTIR analysis

In this work, the annealing temperatures were set to room temperature, 100 °C, and 230 °C. Before deciding on the time of annealing, it should be confirmed that the structure of MEH-PPV was not destroyed under the selected annealing temperatures and times.

Fig. 1 shows the FTIR spectra of pure MEH-PPV, hy-W4, and hy-W200 with annealing at 230 °C for different times. Fig. 1a–c shows that the structure of MEH-PPV remained the same with annealing for 1 h; but significant changes were observed with annealing for 2 h, in which the FTIR bands of ∅-(OCH_3) vibration disappeared. So, in this study, the annealing time was set 1 h.

Another interesting result can also be observed from Fig. 1d and e, which show that almost the entire TIP had been transformed to titania with annealing at 230 °C for 1 h. Moreover, the characteristic band of (RO)–CH_2 asymmetric vibration at 1460 cm^{-1} of MEH-PPV recovered. In our previous study, the disappearance of (RO)–CH_2 vibration of MEH-PPV at 1460 cm^{-1} was assigned to identify the interaction between MEH-PPV and TIP, which occurred at O atom of the 2-ethylhexyloxyl side chain [4]. This means that the properties of MEH-PPV are not restricted by the interaction between MEH-PPV and TIP. For hy-W200, because almost the entire TIP of hy-W200 was converted to titania in the sol–gel reaction, this annealing treatment did not really facilitate the conversion of TIP to titania.

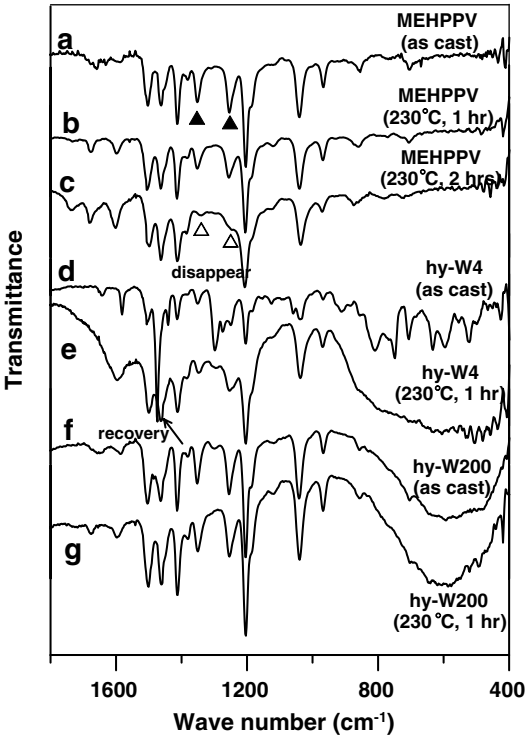

Fig. 1. FTIR spectra of pure-MEHPPV (a), pure-MEHPPV annealed at 230 °C for 1 h (b), pure-MEHPPV annealed at 230 °C for 2 h (c), hy-W4 (d), hy-W4 annealed at 230 °C for 1 h (e), hy-W200 (f), and hy-W200 annealed at 230 °C for 1 h (g).

But this annealing treatment for hy-W200 increased the crystallinity of the titania, which is discussed in the section of XRD analysis.

3.2. SEM photographs

The particle size and distribution of TIP (titania) in the MEH-PPV/TIP (titania) hybrid films can be observed on the SEM photographs. Fig. 2a–d shows the morphology of MEH-PPV and hybrids. Clearly, homogenously and evenly distributed hybrid films were obtained from hy-W4 and even hy-W16. The particle size of TIP (titania) was about 10 nm. The amount of TIP in hybrid, 60.3 wt%, was comparable with that of MEH-PPV. Therefore, the entire TIP had strong interactions with MEH-PPV. Thus the sol–gel reaction was rather slow to be able to maintain the homogenous morphology. But in the hy-W200 hybrid, the sol–gel reaction was too fast in the presence of large amount of water. Therefore the aggregation of titania and phase separation were observed, as shown in Fig. 2d.

It should be claimed that the applicable inorganic material used for application in electro-optical

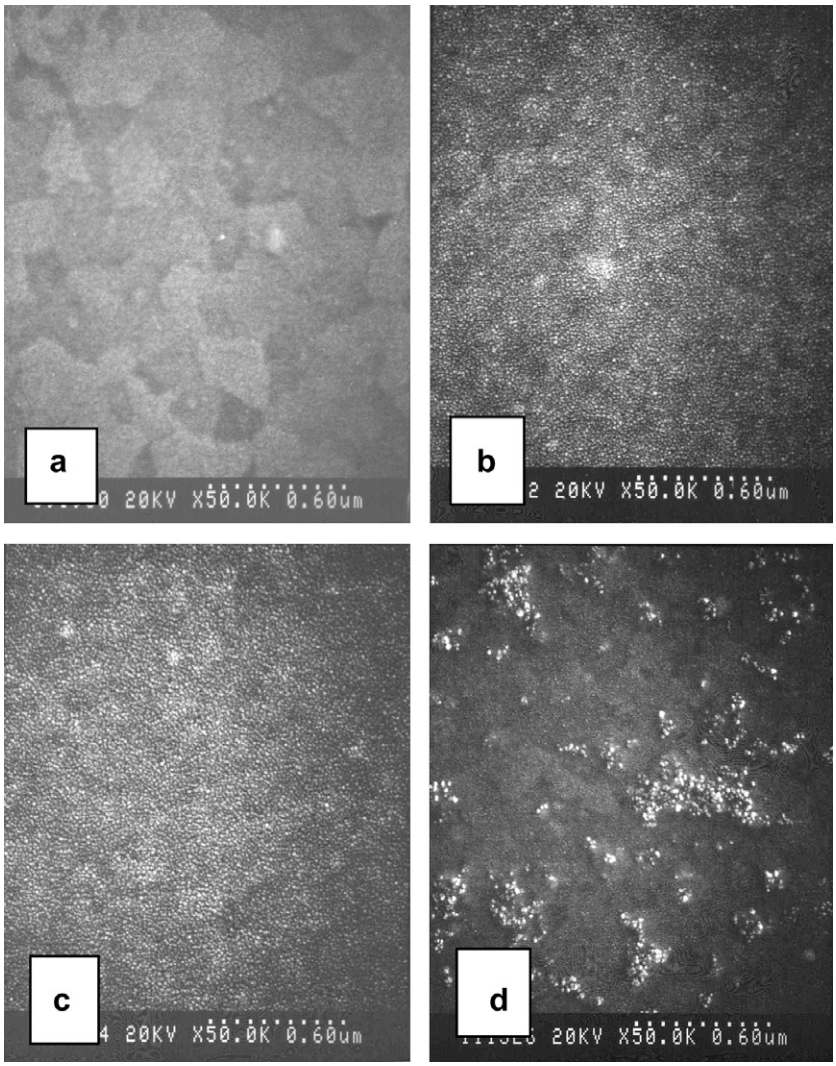

Fig. 2. SEM photographs of pure MEH-PPV and hybrid films prepared with different amounts of water, pure MEH-PPV (a), hy-W4 (b), hy-W16 (c), and hy-W200 (d).

devices is titania not TIP. With an appropriate amount of water, homogenous hybrid films can be prepared, but the conversion of TIP to titania was not complete. Therefore, annealing treatment was necessary and important for the further conversion of TIP to titania as described in the FTIR analysis. This annealing process at 230 °C for 1 h produced homogenous and applicable MEH-PPV/titania hybrid films.

3.3. Thermal analysis

The thermal properties of the organic/inorganic hybrids were measured by TGA under a nitrogen atmosphere. Fig. 3 shows the thermal degradation behaviors of pure MEH-PPV and hy-W4. It reveals that the thermal stability of pure MEH-PPV slightly decreased after the annealing treatment. Although annealing at 230 °C for 1 h did not destroy the main structure of MEH-PPV as seen from the FTIR results, it may have caused some decomposition of MEH-PPV chains and thereby lowered its overall thermal stability. But for hybrid, it indicated that annealing treatment improved the thermal stability. Most of the weak functional groups, such as Ti–OR and Ti–OH, were converted to stronger Ti–O–Ti bonds during the annealing treatment. As to the residual weight of the hybrids, results revealed that

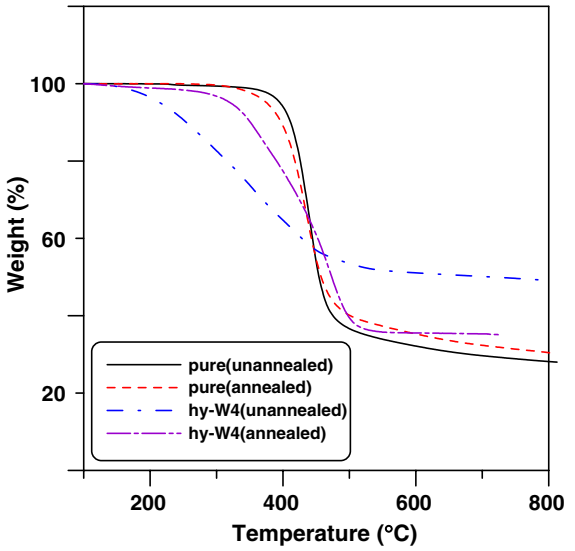

Fig. 3. Thermal degradation behavior of pure MEH-PPV and hy-W4 before and after annealing treatment.

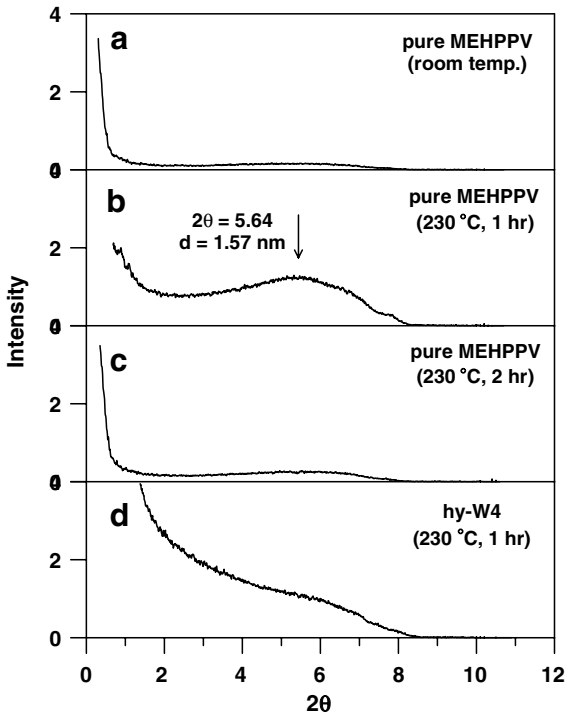

Fig. 4. Small angle X-ray scattering of pure MEH-PPV and hy-W4: MEH-PPV annealed at room temperature (a), MEH-PPV annealed at 230 °C for 1 h (b), MEH-PPV annealed at 230 °C for 2 h (c), and hy-W4 annealed at 230 °C for 1 h (d).

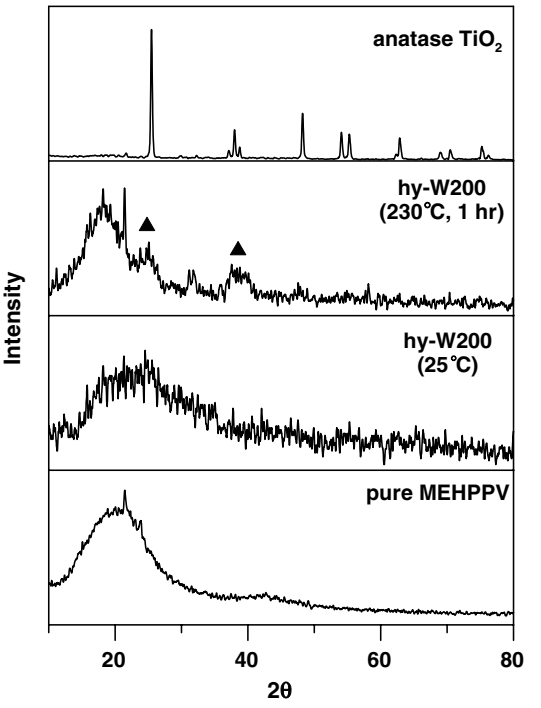

Fig. 5. X-ray diffraction patterns of pure MEH-PPV, anatase form of TiO_2, and hy-W200 before and after annealing treatment.

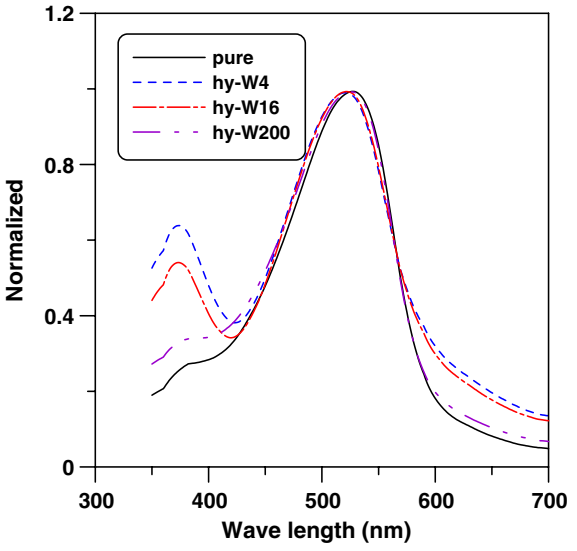

Fig. 6. UV–vis absorption spectra of pure MEH-PPV and hybrid films in a solid state. Results were normalized based on λ_{max} of MEH-PPV.

the residual weights decreased after the annealing treatment. This can be attributed to two causes. First, after annealing, the weight content of the inorganic component of the annealed hybrid was relatively lower than that of the un-annealed hybrid because the groups of Ti–OR and Ti–OH were transformed to Ti–O–Ti, and R–OH/H_2O was

released during annealing. Second, the interaction between MEH-PPV and TIP (titania) decreased after the annealing treatment, and the enhancement effect of titania on the thermal property of MEH-PPV decreased.

3.4. SAXS and XRD analyses

Fig. 4a–d shows the SAXS of pure MEH-PPV and hy-W4 after the annealing treatment, respectively. After annealing treatment, a broad peak of around $2\theta = 5.6$ had developed. This indicated that the MEH-PPV chains were in an ordered arrangement to a certain extent with a *d*-spacing of about 1.57 nm after the annealing treatment at 230 °C for 1 h. When the annealing time was increased to 2 h, this broad peak dissipated, which is consistent with the degradation of the structure obtained from the FTIR analysis. Fig. 4d shows the SAXS of the hy-W4 hybrid, which exhibits no peak. This confirms that the arrangement of MEH-PPV chains was confined by nearby TIP (titania), which resulted in a negligibly ordered arrangement.

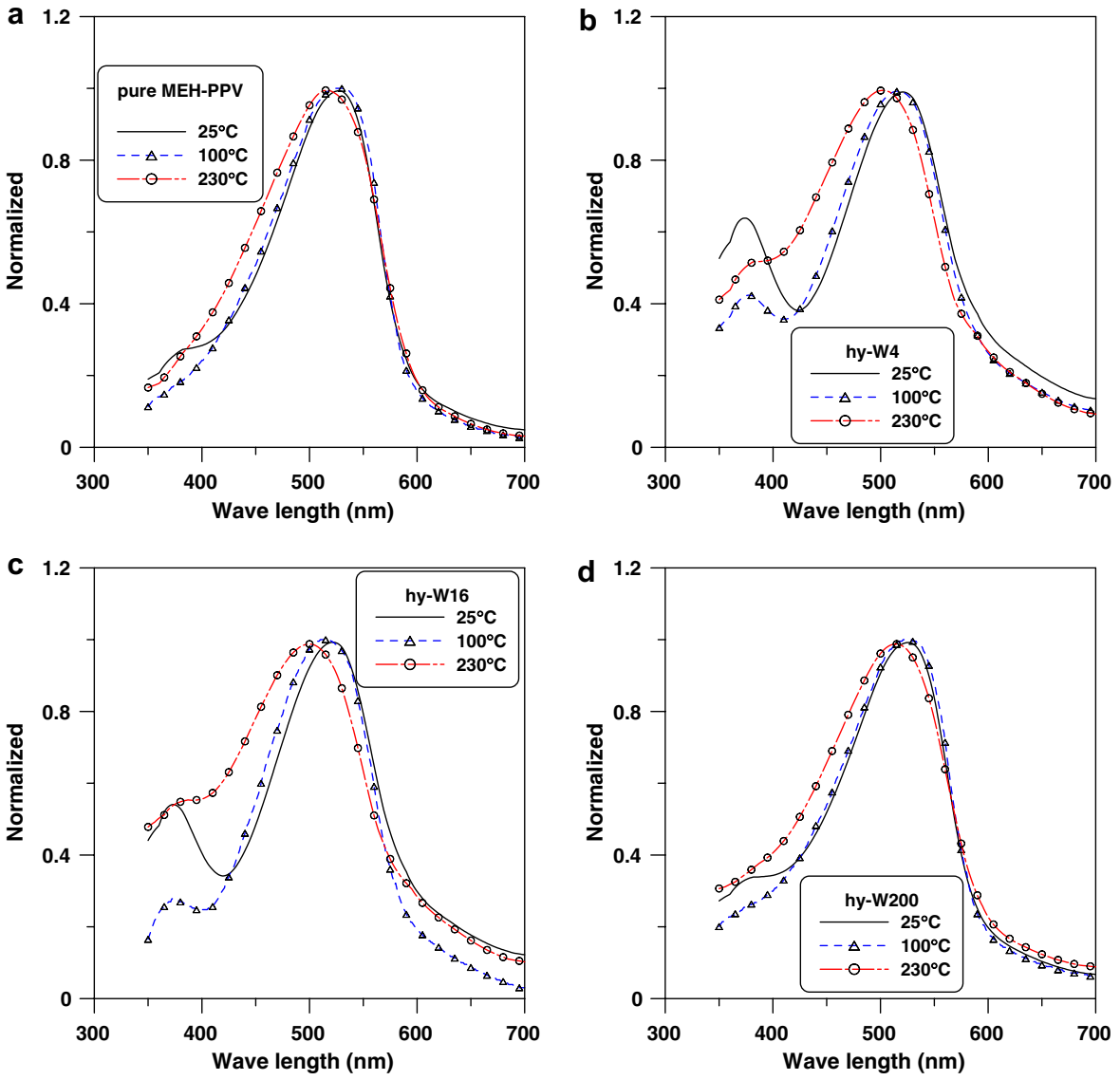

Fig. 7. Effect of annealing temperature on the UV–vis absorption spectra of films: pure MEH-PPV (a), hy-W4 (b), hy-W16 (c), and hy-W200 (d). Results were normalized based on λ_{max} of MEH-PPV.

Fig. 4 shows the effects of annealing treatment on the molecular arrangement of MEH-PPV. But, the crystallinity of titania after the annealing treatment can best be illustrated by wide-angle X-ray diffraction (XRD), as shown in Fig. 5. Fig. 5 clearly exhibits that the crystallinity of titania in the hy-W200 hybrid increased after the annealing treatment. This annealing treatment is an important process for converting TIP to titania and increasing its crystallinity. The main purpose of this treatment was to prepare an applicable MEH-PPV/titania hybrid.

3.5. UV–vis analysis

Fig. 6 shows the UV–vis absorption of pure MEH-PPV and hybrid films. It was normalized based on the λ_{max} of MEH-PPV. Hybrids showed a slight blue shift compared to pure MEH-PPV. In the hybrid, the aggregation (π–π stacking) of the MEH-PPV chains was interrupted by nearby TIP (titania). In addition, TIP (titania) served as a heterogeneous point, which induced the coiled form of the MEH-PPV chains. Both of these effects resulted in a lower conjugation length of MEH-PPV.

Fig. 7a–d shows the effects of annealing temperature on the UV–vis absorption of pure MEH-PPV and hybrid films. Fig. 7a shows the effect of annealing treatment on the UV–vis absorption of pure MEH-PPV. With annealing at 100 °C for 1 h, the UV–vis absorption peak became broader. From the literature, the glass transition temperature of MEH-PPV is about 70 °C [6,29]. During the annealing process, MEH-PPV chains begin to move and migrate. This resulted in a certain extent of ordered and disordered aggregations. These aggregations caused the conjugation length of MEH-PPV to be broader. When the annealing temperature was increased to 230 °C, Fig. 7a shows that the broader peak was blue-shifted. This suggests that although the structure of MEH-PPV was not destroyed with annealing at 230 °C for 1 h, some of the MEH-PPV chains had decomposed, as shown in the TGA analysis. This indicates that the main conjugation length of MEH-PPV was unchanged, but some lower-M_w MEH-PPV were produced. Hence, the position at the longer wavelength was similar but the position at the shorter wavelength was blue-shifted. Of course, except for the decomposition, this higher annealing temperature also promoted coil formation, disordered aggregation, and ordered aggregation of the MEH-PPV chains. As discussed under the SAXS and XRD analyses, MEH-PPV has a certain extent of ordered aggregation with annealing at 230 °C for 1 h even though it was not significant. In general, this annealing treatment decreased the conjugation length of MHE-PPV but retained a certain extent of ordered aggregation.

As seen from Fig. 7b and c, the blue shift of the hybrid films was more obvious after annealing at 230 °C for 1 h. This was due to the fact that the interaction between TIP and MEH-PPV decreased after annealing at 230 °C for 1 h from the FTIR analysis, aggregation of the MEH-PPV chains was easier, and they were not strongly confined by TIP. But the existence of heterogeneous points, titania (TIP), gave rise to a coiled conformation and irregular aggregations of the MEH-PPV chains. The conjugation length of MEH-PPV decreased. So, the blue shift in the absorption was more obvious for the hy-W4 and hy-W16 hybrids. The ordered aggregation of MEH-PPV under the annealing treatment was difficult to obtain for the hybrids as discussed under the SAXS analysis. But for the hy-W200 hybrid, as shown in Fig. 7d, because there was an obvious phase separation between MEH-PPV and titania, the aggregation behavior of MEH-PPV chains recovered to the behavior of pure MEH-PPV and the influence of titania was minor.

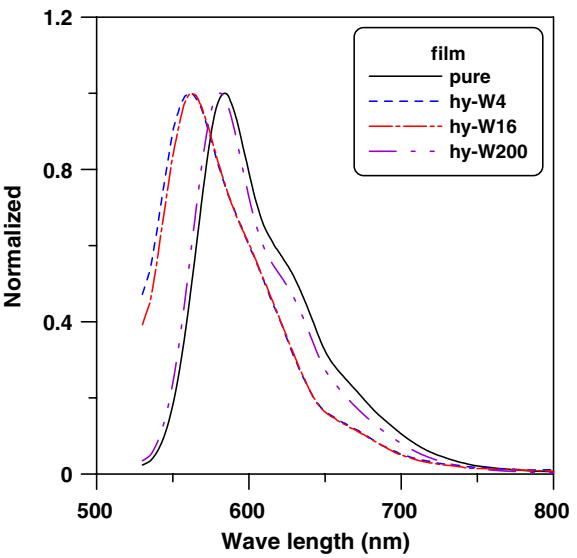

Fig. 8. Effect of the amount of water on the PL emissions of the hybrid films. Results were normalized based on λ_{max} of MEH-PPV.

3.6. PL analysis

3.6.1. Effect of the amount of water on the PL

Fig. 8 shows the effect of water amount on the PL emissions of pure MEH-PPV and hybrid films. In the hy-W4 and hy-W16 hybrids, TIP (titania) was evenly dispersed in the MEH-PPV film, and strong interactions existed among them. The interchain interactions of MEH-PPV were interrupted by TIP (titania). The reduction in interchain interactions resulted in a blue shift of the PL emission [30]. The PL behavior of the hy-W200 hybrid tended to reveal the PL emission of pure MEH-PPV due to the apparent phase separation.

3.6.2. Effect of annealing treatment on the PL

Fig. 9a–d shows the effect of the annealing treatment on the PL emissions of pure MEH-PPV and the hybrid films, which were normalized based on the λ_{max} of MEH-PPV. As can be seen, increasing the annealing temperature dramatically varied the shape of the emissions: broader and red-shifted for pure MEH-PPV and the hy-W200 hybrid. It is known that the emission peaks of pure MEH-PPV

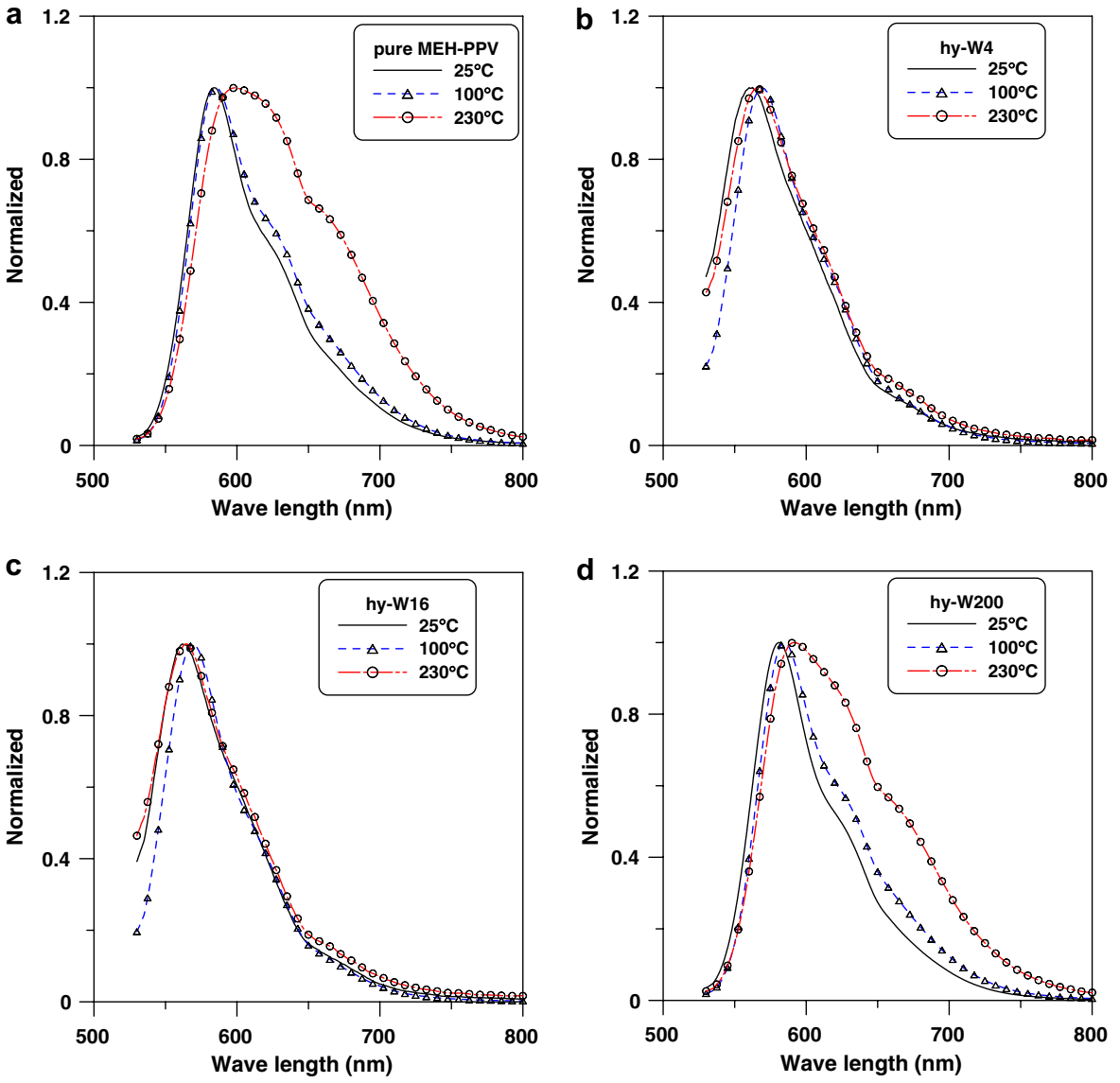

Fig. 9. PL emissions of MEH-PPV and MEH-PPV/TIP (titania) hybrid films under different annealing temperatures: room temperature, 100 °C, and 230 °C; pure MEH-PPV (a), hy-W4 (b), hy-W16 (c), and hy-W200 (d).

at ~580 and ~625 nm are ascribed to a single-chain (or intrachain) exciton emission and interchain (or aggregation or excimer) emission [5,9,10]. This indicates that the annealing treatment promoted the aggregation of MEH-PPV chains, and the degree of aggregation increased as the annealing temperature increased. As stated in the UV–vis section, the T_g of MEH-PPV was about 70 °C, and these 100 and 230 °C annealing temperatures helped the MEH-PPV chains move and migrate. This caused a certain extent of ordered aggregation. These ordered aggregations had lower band gaps and served as lower-energy steps. When the energy was absorbed by the decomposed or coiled MEH-PPV chains, which have higher energy band gaps, the energy was transferred to or absorbed by these lower energy steps, and a red-shifted light was emitted. This mechanism suggests that these ordered

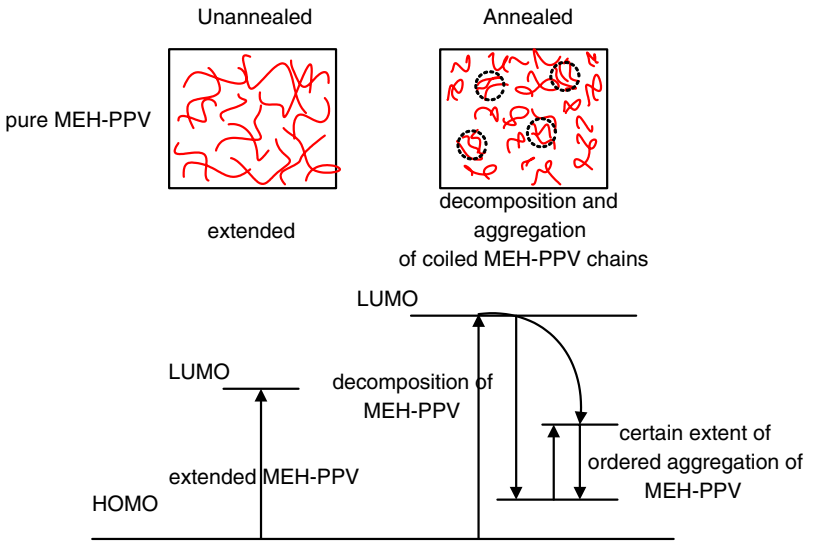

Scheme 1. Chain conformation and energy band gap diagram of pure MEH-PPV before and after annealing.

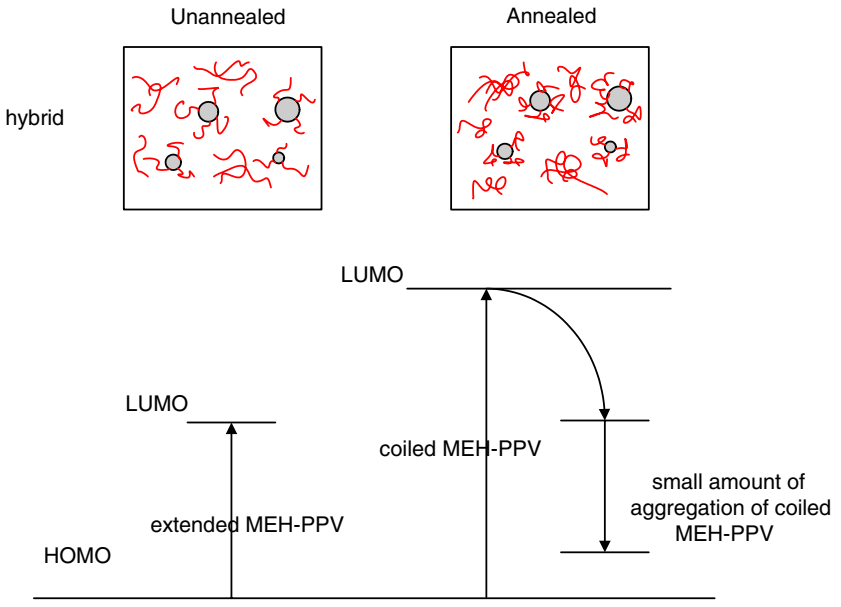

Scheme 2. Chain conformation and energy band gap diagram of hybrids before and after annealing.

aggregations work as funnels of excitation energy by a continuous resonance energy transfer from single-chromophore excitons of disordered chains [14]. Although the extent of the ordered arrangement was not dominant, it had an amplifying effect and controlled the properties of the PL emissions, thus producing the funnel effect. So the emissions of MEH-PPV became broader and apparently red-shifted. The schematic chain conformation and energy transfer diagram are depicted in Scheme 1.

But the hy-W4 and hy-W16 hybrids showed no obvious changes in their emission shapes after annealing, as indicated in Fig. 9b and c. This was because the interactions between MEH-PPV and TIP were relatively strong, which resulted in confinement of the ordered aggregations of MEH-PPV chains. Although the interactions decreased and the degree of aggregation increased after annealing, as stated in the section on the UV–vis analysis, this aggregation was mostly of an irregular form and resulted in an obvious blue shift in UV–vis absorption. This cannot serve as a lower-energy step. Lacking such lower-energy steps, no obvious red shift in the PL emission was observed. Even if ordered aggregations had formed, the amount was too little to contribute to the SAXS and UV–vis measurements. Not until MEH-PPV and titania underwent apparent phase separation, such as in the hy-W200 hybrid, did the PL behavior of the aggregation induced by annealing recover to pure MEH-PPV. Similarly, the schematic chain conformation and energy transfer diagram for the hy-W4 and hy-W16 hybrids are depicted in Scheme 2.

4. Conclusions

A series of MEH-PPV/titania hybrids was prepared using a simple one-step method from MEH-PPV and TIP in the presence of 2-CP solvent via *in situ* sol–gel reaction under ambient condition, followed by annealing treatment. The FTIR analysis indicated that almost the entire TIP was converted to titania, and all characteristic peaks of MEH-PPV recovered after annealing. So, useful and homogenous MEH-PPV/titania hybrid films can be obtained with an appropriate amount of water and annealing treatment, as seen in the results of the FTIR and SEM photographs. The thermal stability of hybrid and crystallinity of titania were improved by annealing as seen from the TGA and XRD results. The annealing treatment of 230 °C for 1 h resulted in a small extent of decomposition and ordered aggregation of MEH-PPV chains. The blue shift of UV–vis absorption for pure MEH-PPV was mainly ascribed to the partial decomposition and coiled conformation; the broader, red-shifted PL emission peak was attributed to a certain extent of ordered aggregation. As for the hybrids, the more-obvious blue-shifted UV–vis absorption may have been due to the coiled form and irregular aggregation of MEH-PPV chains induced by the existence of heterogeneous points, TIP (titania). On the other hand, these heterogeneous points confined the ordered aggregation of MEH-PPV chains and resulted in no obvious changes in the emission peaks. The annealing treatment was efficient for a further conversion of TIP to titania for preparing homogenous MEH-PPV/titania hybrid films. The current study showed that this *in situ* sol–gel reaction with subsequent annealing treatment has the potential to prepare MEH-PPV/titania hybrid films with good thermal and electro-optical properties.

Acknowledgements

The authors would like to thank the Instrumentation Center, National Taiwan University, and Ching-Yen Lin and Chih-Yuan Tang for the use of SEM.

References

[1] Roux S, Soler-Illia GJAA, Demoustier-Champagne S, Audebert P, Sanchez C. Adv Mater 2003;15(3):217–21.
[2] Schnitzler DC, Meruvia MS, Hümmelgen IA, Zarbin AJG. Chem Mater 2003;15(24):4658–65.
[3] Chiang PC, Whang WT. Polymer 2003;44(8):2249–54.
[4] H.J. Chen, Ph.D. Dissertation, January 2006, National Taiwan University Library, Taiwan.
[5] Shi Y, Liu J, Yang Y. J. Appl. Phys. 2000;87:4254.
[6] Liu J, Guo TF, Yang Y. J. Appl. Phys. 2002;91:1595.
[7] Nguyen TQ, Martini IB, Liu J, Schwartz BJ. J. Phys. Chem. B 2000;104:237.
[8] Kemerink M, van Duren JKJ, van Breemen AJJM, Wildeman J, Wienk MM, Blom PWM, et al. Macromolecules 2005;38:7784.
[9] Chen SH, Su AC, Chou HL, Peng KY, Chen SA. Macromolecules 2004;37:167.
[10] Jeng U, Hsu CH, Sheu HS, Lee HY, Inigo AR, Chiu HC, et al. Macromolecules 2005;38:6566.
[11] Friends RH, Gymer RW, Holmes AB, Burroughes JH, Marks RN, Taliani C, et al. Nature 1999;397:121.
[12] Jenekhe SA, Osaheni JA. Science 1994;265:765.
[13] Inigo AR, Tan CH, Fann WS, Huang YS, Perng GY, Chen SA. Adv Mater 2001;13:504.

[14] Chen SH, Su CH, Su AC, Chen SA. J Phys Chem B 2004;108:8855.
[15] Weinfurtner KH, Fujikawa H, Tokito S, Taga Y. Appl Phys Lett 2000;76:2502.
[16] Yan L, Yang F. J Polym Sci Part B: Polym Phys 2005;43:1382.
[17] Kulkarni AP, Jenekhe SA. Macromolecules 2003;36:5285.
[18] Xiao S, Nguyen M, Gong X, Cao Y, Wu H, Moses D, et al. Adv Funct Mater 2003;13:25.
[19] Chou CH, Hsu SL, Yen SW, Wang HS, Wei KH. Macromolecules 2005;38:9117.
[20] van Breemen AJJM, Herwig PT, Chlon CHT, Sweelssen J, Schoo HFM, Benito EM, et al. Adv Funct Mater 2005;15:872.
[21] Yang X, van Duren JKJ, Janssen RAJ, Michels MAJ, Loos J. Macromolecules 2004;37:2151.
[22] Zhong H, Yang X, deWith B, Loos J. Macromolecules 2006;39:218.
[23] van Hal PA, Wienk MM, Kroon JM, Verhees WJH, Slooff LH, van Gennip WJH, et al. Adv Mater 2003;15:118.
[24] Slooff LH, Kroon JM, Loos J, Koetse MM, Sweelssen J. Adv Funct Mater 2005;15:689.
[25] Beek WJE, Slooff LH, Wienk MM, Kroon JM, Janssen RAJ. Adv Funct Mater 2005;15:1703.
[26] Okuya M, Nakade K, Kaneko S. Sol Energy Mater Sol Cells 2002;70:425.
[27] Pichot F, Pitts JR, Gregg BA. Langmuir 2000;16:5626.
[28] Kim H, Auyeung RCY, Ollinger M, Kushto GP, Kafafi ZH, Pique A. Appl Phys A 2006;83:73.
[29] Lee TW, Park OO. Adv Mater 2000;12:801.
[30] Qi D, Kwong K, Rademacher K, Wolf MO, Young JF. Nano Lett 2003;3:1265.